Jarrett-Wilkins, C., He, X., Symons, H., Harniman, R., Faul, C. FJ., & Manners, I. (2018). Living Supramolecular Polymerisation of Perylene Diimide Amphiphiles by Seeded Growth under Kinetic Control. *Chemistry - A European Journal*. https://doi.org/10.1002/chem.201801424

CHEMISTRY
A European Journal

A Journal of
ChemPubSoc Europe

Accepted Article

Title: Living Supramolecular Polymerisation of Perylene Diimide Amphiphiles by Seeded Growth under Kinetic Control

Authors: Charlie Jarrett-Wilkins, Xiaoming He, Robert L. Harniman, Charl F. J. Faul, Ian Manners, and Henry Symons

To be cited as: *Chem. Eur. J.* 10.1002/chem.201801424

Link to VoR: http://dx.doi.org/10.1002/chem.201801424

Supported by
ACES

WILEY-VCH

10.1002/chem.201801424

WILEY-VCH

Living Supramolecular Polymerisation of Perylene Diimide Amphiphiles by Seeded Growth under Kinetic Control

Charles Jarrett-Wilkins,[a] Xiaoming He,[b] Henry E. Symons,[a] Robert L. Harniman,[a] Charl F. J. Faul,[a]* Ian Manners[a]*

Abstract: We demonstrate the controlled solution self-assembly of an amphiphilic perylene diimide (PDI), with a hydrophobic perylene core and hydrophilic imide substituents with polydisperse oligo(ethyleneglycol) (OEG) tethers. It was possible, by a seeded-growth mechanism, to form colloidally stable, one-dimensional fibres with controllable lengths (from 400 to 1700 nm) and low dispersities (1.19-1.29) via a living supramolecular polymerisation process. Under the solvent conditions employed, it was found that molecularly dissolved material (unimer) was present in samples of the fibre-like supramolecular assemblies. The free unimer may be present in a conformationally derived kinetically trapped state and/or may represent a more soluble PDI fraction with longer hydrophilic tethers. Significantly, it was also possible to form segmented supramolecular block copolymers by the addition of PDI unimer to chemically distinct PDI seeds, yielding fibres with controlled lengths. These results represent a significant advance in the ability to form PDI-based supramolecular polymers with precisely controlled lengths and architectures.

Introduction

The ability of small molecules to hierarchically self-assemble via non-covalent interactions into supramolecular polymers has developed into an important field in materials chemistry.[1] The monomer units form reversible and directional bonds, producing supramolecular structures with defined repeat units. Supramolecular polymers are usually 'dynamic' in nature due to the reversible, weak non-covalent interactions between monomer units. This dynamic nature leads to interesting possibilities for application and further exploration, including self-healing materials,[1g] transient assemblies[2] and self-replicating systems with the potential ability to evolve.[3]

Supramolecular polymers can form by two main mechanisms; isodesmic and cooperative growth.[1a] Isodesmic growth is characterised by the energetically identical, reversible formation of a non-covalent bond at each step of the polymerisation, analogous to step-growth covalent polymerisation which, in contrast, generates 'static' materials. For cooperative growth, initial nucleus formation is more thermodynamically unfavourable than subsequent fibre elongation. In this case nuclei form slowly and elongation occurs rapidly,[1a, 1d, 1e] and, until full conversion, a bimodal distribution consisting of monomers and polymers with a high degree of polymerisation is maintained.[1a] This type of process is analogous to a chain-growth covalent polymerisation. Three criteria have been specified[4] for distinguishing cooperative from isodesmic growth: (a) the supramolecular polymerisation has an associated time lag, (b) this lag-time can be removed by the addition of preformed nuclei (termed seeds) and (c) there is a critical temperature or concentration at which polymer elongation occurs.

Perylene diimides (PDIs) have gained widespread interest as building blocks for supramolecular polymers via solution self-assembly. These molecules offer attractive optoelectronic properties to facilitate the study of their self-assembly, easy chemical modification, and wide-ranging potential applications.[1f, 5] PDIs can aggregate in a face-on-face manner via π-π and hydrogen-bonding interactions into spherical micelles,[6] vesicles,[6-7] ribbons,[8] fibres,[9] nanotubes[10] and more complex two-dimensional structures.[11] PDI assemblies exhibit n-type semiconducting behaviour, making these materials of interest for organic electronics and photovoltaic applications.[12] In addition, their co-assembly with other nanostructures is of interest for the formation of p–n nanoheterojunctions.[13] The ability to control the self-assembly of PDIs is important, as regulating the length and width of these fibres could impart uniform behaviour, increase the long-term colloidal stability, and may also provide a way to modulate their optoelectronic properties (as recently shown for block copolymer (BCP) fibre-like micelles).[14]

Due to the tendency for small molecules to form structures that are dynamic in nature (i.e., where the building blocks can exchange between an aggregated and molecularly dissolved or unimeric state), there are relatively few examples of the controlled growth of supramolecular polymers. By suppressing this dynamic nature, supramolecular polymerisations could potentially occur via a living mechanism under kinetic control. This would.be analogous to a living covalent polymerisation of molecular monomers in which a chain growth mechanism occurs with rapid initiation and no chain transfer or chain termination. Control over the length and architecture of supramolecular polymers would therefore be possible.[1h, 15]

Over the past decade, length control of one-dimensional colloidal structures has been achieved by the solution self-assembly of block copolymers (BCPs) with a crystallisable core-forming block.[16] The use of solvents that are selective for the corona-forming block produces long, polydisperse fibre-like

[a] Dr. C. Jarrett-Wilkins, Henry E. Symons, Dr. R. L. Harniman, Prof. C. F. J. Faul, Prof. I Manners
School of Chemistry
University of Bristol
Cantock's Close, Bristol, BS8 1TS, United Kingdom
E-mail: charl.faul@bristol.ac.uk, ian.manners@bristol.ac.uk,
[b] Prof. X. He
School of Chemical Science and Engineering
Tongji University
1239 Siping Rd., Shanghai, China. 200092

Supporting information for this article is given via a link at the end of the document.

micelles with crystalline cores. Sonication of these long, polydisperse structures causes fragmentation of the crystalline core and forms short seed-like micelles,[17] which can be used as nuclei for epitaxial growth upon addition of further unimer. The use of seeds allows for the slow nucleation process to be circumvented as the unimer can add epitaxially to the exposed crystal faces at the termini of the seeds. This addition leads to cylindrical micelles forming with controlled lengths and low dispersities via a process termed living crystallisation-driven self-assembly (CDSA).[16d] The CDSA process has similarities with a supramolecular polymerisation as the interactions between each BCP within the micelle are non-covalent, directional, and potentially reversible, although the assemblies exist in a kinetically trapped state.[15c]

Seeded- growth approaches to supramolecular polymers, i.e. living supramolecular polymerisation, analogous to the methodology developed for BCP micelles with crystalline-cores, has recently been successfully achieved. For example, the growth of supramolecular heterojunctions by the sequential seeded growth of chemically distinct hexabenzocoronenes has been demonstrated by Fukushima, Aida, and co-workers.[18] Sugiyasu, Takeuchi et al. have shown that the length of fibres formed by zinc(II) porphyrins can be controlled by adding H-aggregate seeds into J-aggregate kinetically trapped monomer solutions.[19] More recently, we and the de Cola group have demonstrated the seeded growth of amphiphilic planar platinum(II) pincer complexes with controlled lengths of up to 600 nm.[20] Other work has also shown this methodology can be applied to, for example, N-annulated perylenetetracarboxamides[21], azobenzenes,[22] protein nanofibrils,[23] dithiol-functionalised peptide hexamers,[3, 24] naphthalene diimides[25] and N-heterotriangulenes.[26] In recent advances, the groups of Würthner [27] and Che[28] have shown that a seeded growth mechanism can be used to prepare PDI-based supramolecular fibers and nanotubes, respectively. However, although clear evidence for seeded growth was provided in each case, and length control was demonstrated in the case of the nanotubes, dispersities for the resulting 1D PDI assemblies were relatively large. In another significant development, Hayward and co-workers reported the seeded growth of PDI in the presence of poly(3-hexylthiophene), which allows the formation of relatively low dispersity fibers with lengths up to ca. 800 nm and with narrow widths due selective polymer adsorption to lateral crystal faces.[13c] In addition, several recent reports have demonstrated the formation of supramolecular copolymers with block structures.[29]

In this work, we report further developments in the living supramolecular polymerisation of PDI-based monomers through the synthesis and studies of the self-assembly of a PDI species with polydisperse oligo(ethyleneglycol) tethers at the imide position. We demonstrate that seeded growth of these species allows the formation of PDI-based fibers with precisely controlled lengths and low dispersities up to ca. 1700 nm, as well as the formation of more complex segmented supramolecular polymers with controlled lengths up to ca. 1300 nm.

Results and Discussion

Synthesis. PDIs with OEGylated imide substituents have been reported to form stable nanoribbons in water.[30] In addition, the employment of an amide linker has been shown to allow the formation of intra- and inter-molecular hydrogen bonds, which impact the kinetics and thermodynamics for self-assembly of these materials.[27a] We chose to functionalise the imide position with polydisperse OEGylated moieties (average degree of polymerization = 8), introducing amphiphilicity into the molecule so that the imide substituent could be selectively solvated over the perylene core in polar solvents. An amide linkage was used to connect the OEGylated moiety to the perylene core, providing functionality capable of forming intermolecular hydrogen bonds between monomer units within the supramolecular polymers. Employing hydrogen bonds was envisioned to increase the

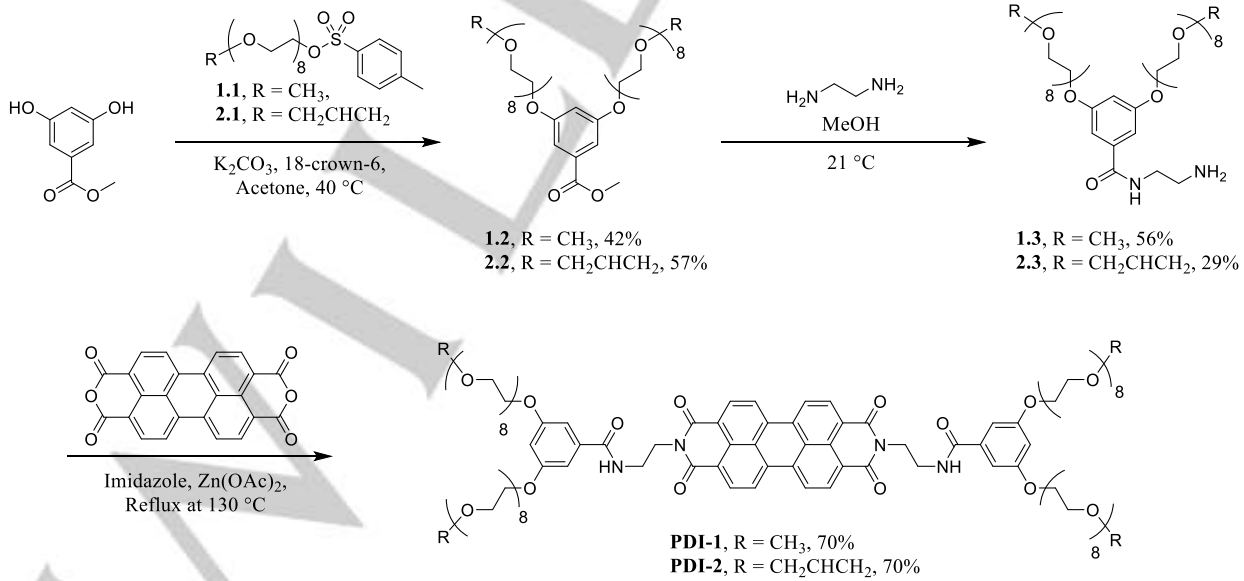

Scheme 1. Synthesis of **PDI-1** and **PDI-2**.

strength of interaction between the monomers and supress dynamic exchange within the supramolecular polymers.

PDI-1 was synthesized by reacting methyl-3,5-dihydroxybenzoate with tosylated-OEG monomethyl ether, **1.1** (average degree of polymerization of the oligo(ethyleneglycol) tethers = 9 by MALDI ToF) to give the OEG-functionalised intermediate **1.2**. Reaction of **1.2** with ethylene diamine introduced a free amine to the molecule (**1.3**), which could then be reacted with perylene-3,4,9,10-tetracarboxylic dianhydride to afford **PDI-1** in 16% overall yield over 3 steps (Scheme 1). See the Supporting Information for detailed information on the synthesis and characterisation by ^{1}H NMR, ^{13}C NMR and MALDI-ToF mass spectroscopy. Differential scanning calorimetry (DSC) revealed a melt endotherm (T_m) at 142 °C on heating and a crystallisation exotherm (T_c) at a temperature of 120 °C on cooling (Fig. S8), indicating that the bulk material was crystalline.

Self-assembly of PDI-1. Initially, PDI-1 was dissolved in chloroform ($CHCl_3$) to afford a solution of molecularly dissolved unimers as shown by UV-visible absorption spectroscopy (Fig. S20a, black trace), which showed characteristic peaks at 490 and 525 nm for the non-aggregated unimers.[5a] To induce self-assembly, an excess of isopropanol (*i*PrOH) was added to the unimer solution. *i*PrOH is a polar solvent, chosen to favour the solvation of the OEG groups over the perylene core. We chose to use an organic polar solvent rather than water, due to concerns about how using a high surface tension solvent such as water would affect the sonication process used later. Initially, a sample was prepared with a selective solvent:common solvent (*i*PrOH:$CHCl_3$) ratio of 9:1 at 4.7 × 10^{-6} M. An aliquot was prepared for transmission electron microscopy (TEM) imaging by drop-casting the solution onto a carbon-coated copper grid and ageing to allow the solvent to evaporate. Analysis of TEM images revealed the formation of multi-micrometer length fibres (Fig. 1a and S20b and c). UV-vis absorption data was also collected on the sample in 9:1 *i*PrOH:$CHCl_3$, which showed a blue shift in absorption band of ca. 5 nm and the appearance of a new red-shifted peak at 556 nm, which can be attributed to the formation of H-aggregates with rotational displacement of the perylene cores (Fig. S20a, red trace and S27).[5a] Comparison of the UV-vis absorption maximum at 525 nm for the fibre solution in 9:1 *i*PrOH:$CHCl_3$ (Fig. S20a, red trace) and unimeric solution in $CHCl_3$ at the same concentration (Fig. S20a, black trace) allowed us to qualitatively state that the amount of unimer was reduced on addition of *i*PrOH; however, quantitative analysis was not possible due to overlap of the unimer and aggregate peaks. Small spheres could be observed by TEM that could have been formed by PDI-1 unimer upon solvent evaporation; however, no unimer film could be detected (Fig. 1a and S20b and c).

Fourier-transform infrared spectroscopy and cryoTEM were also carried out to investigate the importance of intramolecular H-bonding and the structure of fibres in solution, respectively. However, due to the solvent system in use, neither gave clear information regarding the structures of the fibres (Fig. S56 & S57). Although solution-phase microscopy was not possible, we believe that the aggregation data collected from UV-vis experiments suggests that the fibres observed in the dried-state correlate well to the structures in solution. Future studies will aim to characterize the solution-phase structures.

Atomic force microscopy (AFM) images of the sample on carbon-coated TEM grids (prepared from the same concentration, 4.7 × 10^{-6} M) were also collected. Unfortunately, no fibres could be detected under these conditions, however, on increasing the concentration to 9.4 × 10^{-6} M, well-dispersed fibres were observed, with consistent heights of ca. 3 nm (Fig. 1b and 4). A bimodal distribution of PDI material, i.e. that fibres with high degrees of polymerisation form (as observed by TEM and AFM) while monomer remains in solution (as observed by UV-vis), strongly supports a cooperative growth mechanism for the supramolecular polymer.[31]

Temperature-dependent UV-vis absorption spectra were collected to elucidate the mechanism of supramolecular polymerisation.[31-32] Spectra were obtained at 5 K intervals between 288 K and 333 K (Fig. S21) for a sample at 2.8 × 10^{-5} M in 9:1 *i*PrOH:$CHCl_3$. At 288 K, broad unimer peaks at 490 and 525 nm were detected, in addition to the aggregate peak at 556 nm (Fig. S21, red trace). Conversely, at 333 K, the spectrum showed the characteristic unimer peaks at 490 and 525 nm, with no aggregate peak at 556 nm (Fig. S21, black trace). However, the shoulder of the unimer peak at 525 nm meant that there was a non-zero absorbance value at 556 nm. This phenomenon could also be observed in the UV-vis absorption spectra of unimeric PDI-1 in $CHCl_3$ at this concentration (Fig. S22). The temperature-dependent UV-vis absorption spectra were deconvoluted in order to take into account the shoulder of the unimer peak at 525 nm interfering with the value for the aggregate peak at 556 nm (see Supporting Information for further details, Fig. S23-S26). The degree of aggregation (α) was calculated by taking the intensity of the peak at 556 nm after deconvolution and normalising the data.[32c] A plot of degree of aggregation as a function of temperature produced a non-sigmodal curve (Fig. S26), indicative of a cooperative supramolecular polymerisation. Values of the saturation parameter (α_{sat}), elongation enthalpy (ΔH_e) and elongation temperature (T_e) were obtained by fitting the data for the elongation process at 2.8 × 10^{-5} M and 9.4 × 10^{-5} M with the cooperative model proposed by Smulder et al.[31, 33] (Table S1).

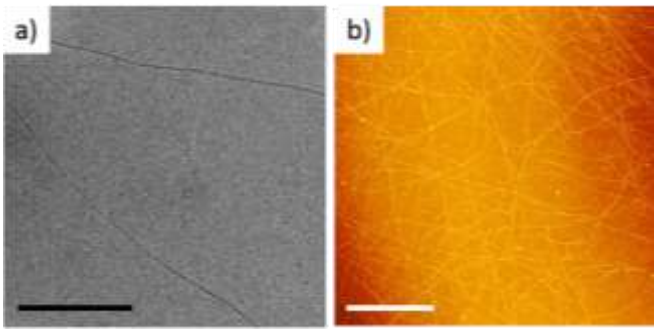

Figure 1. (a) TEM image of fibres formed at 4.7 × 10-6 M in 9:1 iPrOH:CHCl3, (b) AFM height image of fibres formed at 9.4 × 10-6 M in 9:1 iPrOH:CHCl3. Scale bars = (a) 500 nm, (b) 2000 nm.

At 2.8 × 10^{-5} M, values of –20.9 kJmol^{-1} and 318.8 K were obtained for ΔH_e and T_e, respectively. The calculated values of ΔH_e and T_e are significantly smaller than the values reported for the self-assembly of an analogous PDI monomer with alkylated benzyl moieties in methylcyclohexane/toluene (2:1, *v/v*).[27a] It is postulated that *i*PrOH is not a very poor solvent for the PDI-1 unimer, implying that the solvophobic interactions between the monomer units are relatively weak within the supramolecular polymer.

Ideally, the aim was to solely form the aggregated state with no unimer present. Concentration-dependent UV-vis absorption spectra were collected in the range 1.4 × 10^{-6} – 4.7 × 10^{-5} M to determine the concentration at which PDI-1 completely aggregates at room temperature (Fig. S27). As the concentration of the samples was increased, the unimer peaks at 490 and 525 nm became broader and the aggregate peak at 556 nm increased in intensity. The degree of aggregation was taken as the intensity of the aggregate peak at 556 nm relative to the unimer peak at 525 nm,[32c] so that the intensity difference between samples due to concentration could be accounted for (Fig. S27b). Unimer peaks were detectable up to concentrations of 9.4 × 10^{-5} M. Samples at 4.7 × 10^{-6} M, 2.8 × 10^{-5} M, 4.7 × 10^{-5} M and 1.4 × 10^{-4} M in 9:1 *i*PrOH:$CHCl_3$ were analysed by TEM. At 4.7 × 10^{-6} M, fibres were observed which were consistently of very narrow width, ca. 3 nm (Fig. 1a and b). This is slightly larger than the width of the core of PDI-1 when computationally modelled (ca. 2.5 nm, Fig. S9 and S10), probably as a result of the presence of the OEG groups. As the concentration increased (from 4.7 x 10^{-6} to 1.4 x 10^{-4} M), bundling of fibres could be observed alongside the fibres of ca. 4 nm width (Fig. S28).

Alternatively, we expected that reducing the amount of common solvent ($CHCl_3$) would also reduce the amount of free unimer in solution. As anticipated, UV-vis absorption spectroscopy showed a reduced intensity of unimer peaks as the $CHCl_3$ content decreased (Fig. S29a). However, below 10% $CHCl_3$ (by volume), thicker bundles were observed by TEM (Fig. S29c) and below 5% $CHCl_3$, 2D aggregates were present (Fig. S29d).

Next, we explored the use of selective solvent mixtures of *i*PrOH and hexane (rather than using neat *i*PrOH) to increase the degree of aggregation. *i*PrOH and then hexane were added to PDI-1 unimer in $CHCl_3$ at 4.7 × 10^{-5} M, to give a final concentration of 4.7 × 10^{-6} M and selective solvent mixture:common solvent ratio of 9:1. As hexane is a poor solvent for the PDI core, we envisaged that the use of a mixture of *i*PrOH and hexane would lead to a greater degree aggregation. UV-vis absorption spectroscopy showed a decrease in the intensity of the unimer peaks at 525 and 490 nm and an increase of the aggregate peak at 556 nm on increasing the hexane content (Fig. S30a). Using a 1:1 *i*PrOH:hexane selective solvent mixture, consistently thin fibres could be observed by AFM and TEM at 4.7 × 10^{-6} M (Fig. S30c, S31 and S32). As the hexane content in the selective solvent mixture was increased further, the fibres began to bundle (Fig. S30d) and ultimately no individual 1D structures were observed by TEM when 100% hexane was used as the selective solvent (Fig. S30e). It appears that the hydrophilic OEG moiety increased the solubility of the free unimer as well as stabilising the supramolecular polymers in 9:1 *i*PrOH:$CHCl_3$. Attempts to reduce the solubility of the free unimer by changing the solvent conditions led to fibre aggregation in solution due to a reduction in the solubility of the OEG chains.

For controlled growth, we envisaged that using conditions that yield fibres of uniform width would likely be more important than having a completely aggregated state. We therefore explored seeded growth of the fibres formed at 4.7 × 10^{-6} M in 9:1 *i*PrOH:$CHCl_3$.

Seed formation for PDI-1. The fibres formed in 9:1 *i*PrOH:$CHCl_3$ at 4.7 × 10^{-6} M were polydisperse and many micrometres in length (Fig. 1a and b). In order to control the length of the fibres, a seeded-growth method analogous to the living CDSA approach developed for BCPs was employed.[16a, 16c, 16d] Sonication of long, polydisperse fibres caused fragmentation into short seed-like fibres with an average length (L_n) of 65 nm and a significantly lower polydispersity index (L_w/L_n) of 1.17 (Fig. 2a and b and S32). Seed-like fibres could be formed by placing a sonotrode through a septum into a vial containing the fibre solution at 0 °C, with the tip immersed in the solution and sonicating for 10 minutes. Sonication reproducibly formed seeds below 100 nm in length with L_w/L_n values between 1.1 and 1.25. The UV-vis absorption spectrum after sonication revealed a significant increase in the aggregate peak at 556 nm and a reduction in the unimer peaks (Fig. 2c), suggesting PDI-1 molecules had been incorporated into the fibres after sonication.[13c]

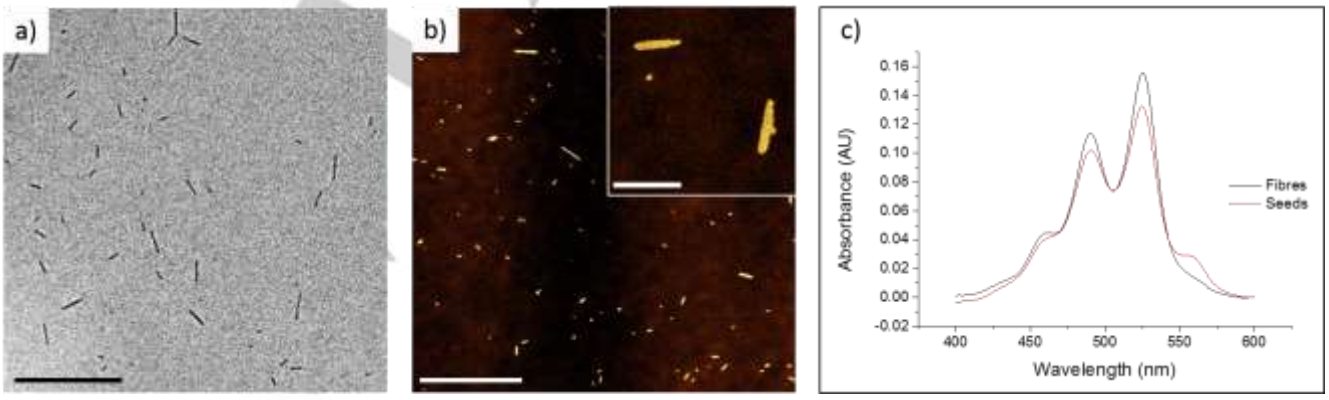

Figure 2. (a) TEM image and (b) AFM height image of PDI-1 seeds in 9:1 iPrOH:CHCl3 at 4.7 × 10-6 M formed by sonication for 10 minutes at 0°C using a sonotrode, (c) UV-vis absorption spectra of the solution before (black trace) and after sonication (red trace). Scale bars = 1000 nm, inset = 200 nm.

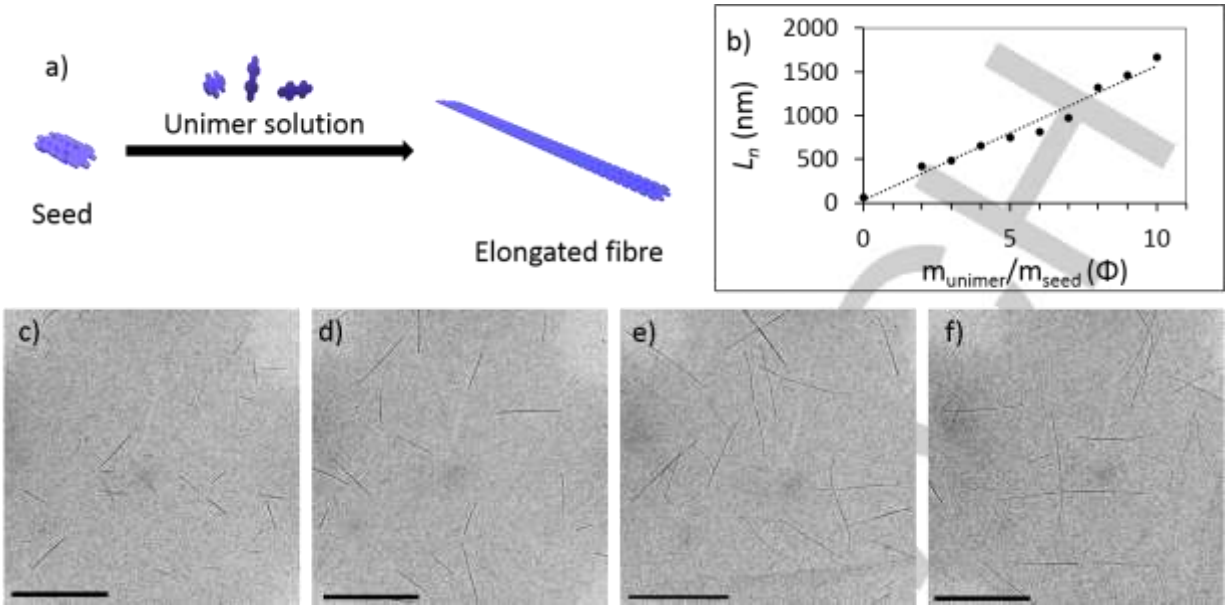

Figure 3. (a) Schematic of seeded growth of PDI-1, (b) Graph showing plot of unimer:seed mass ratio (Φ) vs. average length (Ln) for >200 fibres for each data point, (c)-(f) TEM images showing fibres formed by seeded growth with Φ = (c) 2, (d) 5, (e) 8 and (f) 10 in 9:1 iPrOH:CHCl3 at 4.7 × 10-6 M. Scale bars = 2000 nm.

Kinetic Stability of Seeds of PDI-1. To explore the kinetic stability of the seeds after sonication, the seed solutions in 9:1 *i*PrOH:$CHCl_3$ were left to age and, at specific time intervals, aliquots were taken and imaged by TEM. Analysis of TEM images showed that the seed fibres increased from ca. 80 nm to >300 nm over 24 h (Fig. S34 and S35) and, in addition, seed aggregation was observed after ageing for 24 h (Fig. S35c). Upon sonication, the long fibres fragment into a much larger number of short seed-like fibres. It has previously been shown that for kinetically trapped cooperative supramolecular polymerisation, seeded growth occurs at a much faster rate than formation of new polymers,[19a, 27a] as it is significantly more favourable for unimer in solution to add to preformed aggregates rather than to form new nuclei. It appears that the production of many more nuclei in the solution, by sonication of the long fibres, promotes the seeded growth of free unimer and, in turn, increases the proportion of the aggregated state, as shown by UV-vis absorption spectra (Fig. 2c). Alternatively, sonication may cause a fraction of the molecules associated within the fibres to dissolve, which then re-add to the aggregates after the sonication process.

Seeded growth of PDI-1. It has previously been demonstrated that for the seeded growth of BCP micelles the fibre length is dependent on the mass ratio of added unimer to seeds.[16a, 16d] Seeded growth was attempted using seeds formed by sonication of fibres in 9:1 *i*PrOH:$CHCl_3$ at 4.7 × 10^{-6} M. Immediately after sonication the seeds were diluted in *i*PrOH, and PDI-1 unimer in $CHCl_3$ at 4.7 × 10^{-5} M was added. These conditions were used so that the final concentration was kept constant at 4.7 × 10^{-6} M and the selective solvent:common solvent ratio was maintained at 9:1. We added a range of volumes of the PDI-1 unimer solution in $CHCl_3$ to the seeds, so that the effect of unimer:seed mass ratio (Φ) on L_n could be investigated for values of Φ from 2-10. Analysis of TEM images revealed that a linear relationship was observed between Φ and the L_n of the formed fibres (Fig. 3b), indicating that the growth of PDI-1 unimer from PDI-1 seeds is a living supramolecular polymerisation. TEM images showed that there was no fibre aggregation, even when ca. 1700 nm in length (Fig. 3c-f). All seeded growth experiments produced fibres with low polydispersities between 1.19-1.29 (See Table S2 for values of L_n, L_w, L_w/L_n and standard deviation (σ) and Fig. S37-S45 for TEM images and histograms detailing distribution of fibre lengths for each seeded growth experiment). As previously stated,[27a] the control over the length is expected to only be possible for supramolecular polymers that form by a cooperative growth mechanism, otherwise there would be no preference for the unimer to favour addition to seeds over formation of new polymers.

On ageing the fibres for one month, no change in the morphology was observed (Fig. S46a and b), and no change in the UV-vis spectra occurred after 13 months (Fig. S46c). The supramolecular polymers were fluorescent and could be imaged by laser confocal scanning microscopy (LCSM). Interestingly, the presence of background unimer could not be detected by LCSM; instead, localised areas of fluorescence were observed, which were attributed to the supramolecular polymers (Fig. S47). The resolution of the images was not sufficient for characterisation of the aggregates and future work will focus on improving the experimental conditions for such investigations using super-resolution microscopy techniques.

Height profiles obtained from AFM images provided a value of ca. 3 nm for the fibres formed by seeded growth (Fig. 4i and l), correlating well with that found for the fibres formed by addition of selective solvent to PDI-1 unimer in $CHCl_3$ (Fig. 4c). In

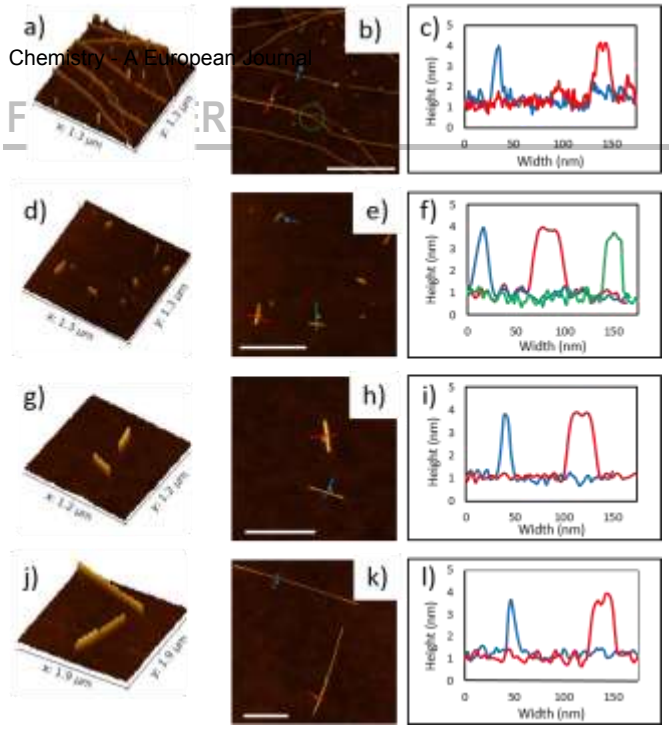

addition, height profiles along the length of the fibres showed the height to be consistent, with no evidence of the original seed or any helicity along the fibre (Fig. S48). Analysis of the widths of the fibres showed that there was a mixture of ca. 10 nm (Fig. 4c, f, i, and l blue traces) and ca. 20 nm wide fibres (Fig. 4c, f, i, and l red traces). This mixture of widths was found for the initial self-assembled fibres, the seeds as well as the fibres formed by seeded growth. AFM height profiles show that for the wider fibres there was evidence of two peaks ca. 3 nm (Fig. 4c, f, i, and l), suggesting that raft-like structures were formed by bundling of the fibres.[34] Indeed, in the AFM images of the initial supramolecular polymers, the intertwining of two fibres could be observed (Fig. 4b, green circle). Interestingly, this bundling was not disrupted by sonication and the seeds retained the width of the bundled fibres. There appeared to be no unimer film present in either TEM or AFM images collected after seeded growth.

Figure 4. (a) 3D AFM image of fibres of PDI-1 in 9:1 iPrOH:CHCl¬3, (b) 2D AFM height image of fibres, (c) Height profiles of fibres, (d) 3D AFM image of seeds of PDI-1 in 9:1 iPrOH:CHCl¬3, (e) 2D AFM height image of seeds, (f) Height profiles of seeds, (g) 3D AFM image of fibres formed by seeded growth at Φ = 2 of PDI-1 in 9:1 iPrOH:CHCl¬3, (h) 2D AFM height image of fibres formed by seeded growth at Φ = 2, (i) Height profiles of fibres formed by seeded growth at Φ = 2, (j) 3D AFM image of fibres formed by seeded growth at Φ = 9 of PDI-1 in 9:1 iPrOH:CHCl¬3, (k) 2D AFM height image of fibres formed by seeded growth at Φ = 9, (l) Height profiles of fibres formed by seeded growth at Φ = 9. Scale bars in b, e, h and k = 500 nm.

It was also of interest to use higher concentration unimer solutions in $CHCl_3$ for the seeded growth, so that the increase in volume of common solvent upon unimer addition to seed solutions could be kept to a minimum. Unfortunately, it was found that as the concentration of unimer increased from 4.7×10^{-5} M to 4.7×10^{-4} M, the structures formed by seeded growth were less well defined, both in terms of width and length (Fig. S49).

Seeded growth was also studied by UV-vis absorption spectroscopy. Spectra collected after the addition of unimer to the seed solution at Φ = 10 showed an increase in the intensity of the aggregate peak at 556 nm with a concurrent reduction in the unimer peaks at 490 and 525 nm (Fig. 5a). The absorbance of the unimer peak at 525 nm decreased after addition of unimer to seeds, alongside an increase in the intensity of the aggregate peak at 556 nm.

The degree of aggregation was calculated by the intensity of the aggregate peak at 556 nm. A normalised plot of the degree of aggregation against time for both seeded growth (Fig. 5b, black squares) and addition of PDI-1 unimer in $CHCl_3$ to *i*PrOH with no seeds present (Fig. 5b, red circles) revealed that the rate of aggregation was much greater when seeds were present. This result clearly indicates that the seeds acted as sites for unimer addition, removing the unfavourable nucleation step and leading to control over the length of structures formed. The elimination of the lag-time of supramolecular polymerisation upon addition of seeds supports the assertion that the growth occurred by a cooperative mechanism.

Accounting for discrepancy between theoretical and experimental fibre length. TEM analysis of the fibres formed by seeded growth revealed that the L_n for each sample was much higher than that expected from the seed length (L_s) and Φ (Eq. 1). L_s was calculated by measuring over 200 seeds from multiple TEM images of samples drop-cast immediately after sonication. Φ was calculated theoretically prior to the seeded growth experiment.

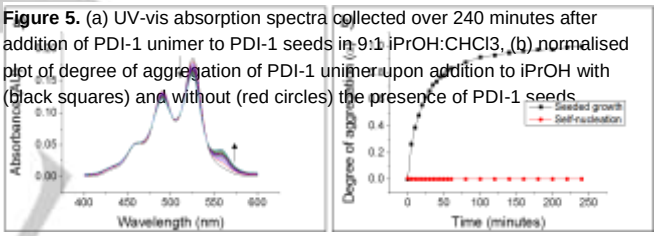

Figure 5. (a) UV-vis absorption spectra collected over 240 minutes after addition of PDI-1 unimer to PDI-1 seeds in 9:1 iPrOH:CHCl3, (b) normalised plot of degree of aggregation of PDI-1 unimer upon addition to iPrOH with (black squares) and without (red circles) the presence of PDI-1 seeds.

$$L_n = L_s(1 + \Phi)$$

As has already been discussed, the UV-vis absorption data showed that, in 9:1 *i*PrOH:$CHCl_3$, not all the PDI-1 molecules aggregate into supramolecular polymers and a significant amount remained as unimer. Previously it has been reported that PDI molecules with an amide linker between the PDI core and benzyl moiety can undergo intramolecular hydrogen-bonding to kinetically trap the monomer.[27a] It is possible that this kinetic trapping partially accounts for the large amount of unimer still present, however, we believe that the very low concentrations employed here may also explain the presence of free unimer. In addition, as the OEG chains have a distribution of lengths, PDIs decorated with longer chains would be better solvated and less likely to aggregate.

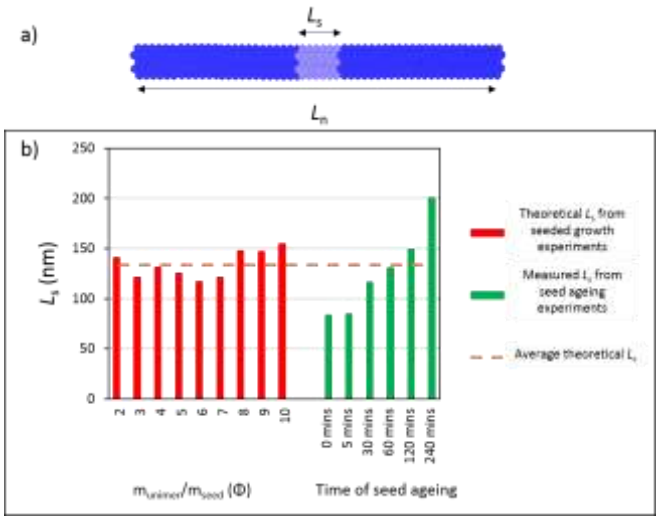

Figure 6. (a) Schematic of a PDI-1 fibre formed by seeded growth indicating the length of seed (Ls) and length of fibre (Ln), (b) Graph showing theoretical values of Ls calculated using known Ln and Φ values from seeded growth experiments (red bars), the average theoretical Ls (dashed orange line) and Ls values for seeds aged for different lengths of time (green bars).

After sonication, an increase in the length of the seeds, from ca. 80 nm to ca. 200 nm, occurred on ageing for 240 minutes (Fig. S34 and S35), which we attributed to growth of free unimer. We then proceeded to investigate whether seeds that had been aged better matched theoretical L_s values from seeded growth experiments (Fig. 3). Theoretical L_s values were calculated from Eq. 1 using known values of L_n and Φ. The green bars in Fig. 6b show values of L_s measured from seed ageing experiments (see also Fig. S34) compared with the theoretical values from seeded growth experiments at each value of Φ (red bars). We found that seeds aged for 60 minutes had the closest match to the average theoretical L_s (dashed orange line). The fact that the increase in L_s on ageing matches well with the theoretical L_s supports the argument that unimer present in the solution added to the seeds upon ageing, leading to an increase in L_s. This subsequently caused the fibres formed by seeded growth to be longer than expected.

The seeded growth experiments described above were also carried out using a selective solvent mixture of 1:1 *i*PrOH:hexane (rather than *i*PrOH in the *i*PrOH/$CHCl_3$ system discussed above). It was found that controlled growth of fibres was possible using this selective solvent mixture, however, the polydispersity of the fibres formed by seeded growth was higher, with values ranging from 1.27-1.65, (see Table S3 for values of L_n, L_w, L_w/L_n and standard deviation (σ), Fig. S50 for plot of L_n vs Φ, Fig. S51 for TEM images of fibres formed in each seeded growth experiment and Fig. S52 for histograms detailing distribution of fibre lengths for each seeded growth experiment).

Formation of segmented fibres. In an attempt to access more complex supramolecular architectures, a second PDI with vinyl-terminated OEG chains, PDI-2, was synthesised (Scheme 1). We followed the same synthetic route as for PDI-1 after initially functionalising one end of a OEG chain with a vinyl moiety. Vinyl groups were introduced at the OEG chain termini with the aim

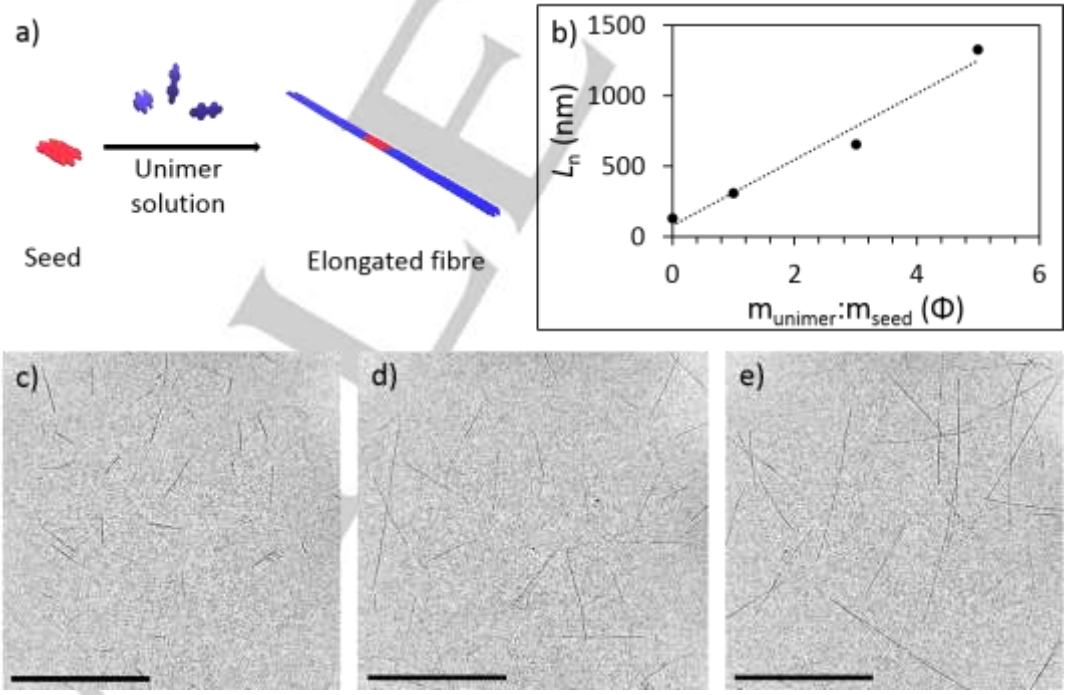

Figure 7. (a) Schematic depicting seeded growth of PDI-1 unimer from PDI-2 seeds, (b) graph showing plot of unimer:seed mass ratio (Φ) vs. average length (Ln), (c)-(e) TEM images showing fibres formed by seeded growth with Φ = (c) 1, (d) 3 and (e) 5 in 10:5:2 iPrOH:hexane:CHCl3. Scale bars = 2000 nm.

that, on formation of supramolecular block co-polymers, staining of the vinyl groups or coordination of nanoparticles could be employed to distinguish the blocks.

The supramolecular polymerisation of PDI-2 gave well-dispersed fibres with consistent widths (Fig. S53) at concentrations of 1.4 × 10^{-5} M in 9:9:2 *i*PrOH:hexane:$CHCl_3$ (as opposed to self-assembly of PDI-1 at 4.7 × 10^{-6} M in 9:1 *i*PrOH:$CHCl_3$). The vinyl group at the termini of the OEG chains appeared to increase the solubility of PDI-2 in *i*PrOH and meant self-assembled structures only formed at higher concentration in mixtures of *i*PrOH and hexane. These fibres could be sonicated using the same conditions as for PDI-1 to give seeds with an L_n of 126 nm and a L_w/L_n value of 1.29.

PDI-2 seeds in 9:9:2 *i*PrOH:hexane:$CHCl_3$ were diluted in 3:1 *i*PrOH:hexane, followed by the addition of PDI-1 unimer at 4.7 × 10^{-5} M in $CHCl_3$, thus forming triblock supramolecular polymers. This approach led to fibres with well-controlled lengths (from ca. 300 to 1320 nm), relatively low polydispersities (1.26-1.38) and consistent widths (Fig. 7c-e), similar to those seen for the seeded growth of PDI-1 unimer from PDI-1 seeds (see Table S4 for values of L_n, L_w, L_w/L_n and standard deviation (σ) and Fig. S55 for histograms detailing distribution of fibre lengths for each seeded growth experiment). Again, there was a linear relationship between the L_n of the fibres and Φ (Fig. 7b), showing that the seeded growth is a living process. Control experiments where PDI-2 seeds were diluted in 3:1 *i*PrOH:hexane showed no fibres by TEM after ageing overnight. The seeded growth of PDI-1 unimer from PDI-2 seeds was also characterised by UV-vis absorption spectroscopy (Fig. 8).

Upon sonication of the fibres, there was a small decrease in the intensity of the unimer peaks, however a significant increase in the aggregate peak at 556 nm was apparent (Fig. 8a). On ageing of the seeded growth experiment for 1380 minutes, there was a reduction in the intensity of the unimer peaks (Fig. 8b), implying that PDI-1 unimer added to and grew from the PDI-2 seeds. Both the reduction in amount of PDI-1 unimer, as well as the controlled structures formed during the seeded growth experiments (Fig. 7b-e) provide strong evidence that segmented block supramolecular polymers are forming due to the addition of PDI-1 unimer from PDI-2 seeds.

Due to the similarity in chemical structure of the two PDI molecules, it was not possible to resolve the different blocks by TEM. Selective staining of the vinyl groups with osmium tetroxide, as well as interactions of the vinyl groups with metal salts and nanoparticles, was attempted. Unfortunately, the segments could not be distinguished by TEM or energy-dispersive X-ray spectroscopy. We believe that the number of reactive vinyl groups was too low for successful characterisation of the supramolecular block copolymers and future work will attempt to incorporate a higher density of vinyl (or other functional) moieties into the structure of PDI-2, for facile differentiation of the blocks.

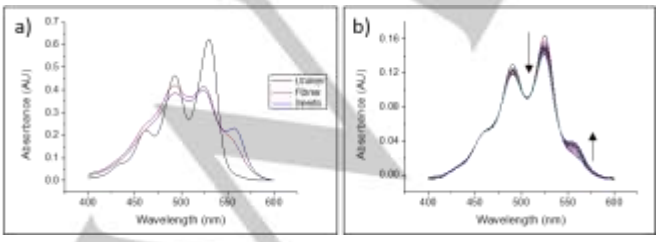

Figure 4. (a) UV-vis absorption spectra of unimeric PDI-2 in CHCl3 at 1.4 × 10-5 M (black trace) and PDI-2 in 9:9:2 iPrOH:hexane:CHCl3 at 1.4 × 10-5 M before (red trace) and after (blue trace) sonication, (b) UV-vis absorption spectra collected over 240 minutes after addition of PDI-1 unimer to PDI-2 seeds in 10:5:2 iPrOH:hexane:CHCl3.

Conclusions

We have shown the seeded growth, living CDSA method developed for BCP micelles with crystalline cores can be applied to a PDI supramolecular polymer to form fibres with control over the length. In the case of **PDI-1**, fibres of up to ca. 1700 nm can be formed with a relatively low dispersity in length (1.19-1.29). We believe this is the first report of the seeded growth of PDIs to form supramolecular polymers with precise control over their lengths which show no signs of bundling. Significantly, there was a linear relationship between L_n and Φ, indicating that the seeded growth of the supramolecular polymers was a living process. Temperature-dependent UV-vis absorption spectra indicated **PDI-1** formed supramolecular polymers by a cooperative growth mechanism, which was supported by (a) a bimodal distribution of supramolecular polymers with a high degree of polymerisation and free unimer in the sample of self-assembled fibres, (b) the removal of the lag time for polymerisation upon addition of seeds and (c) the ability to control the length of the fibres by a seeded growth mechanism.

UV-vis absorption data showed that after addition of selective solvent to **PDI-1** unimer solution both the unimeric species and aggregated species were present. We believe the presence of free unimer in the aggregate solution may have been due to either kinetic trapping of the monomers, the very low concentrations employed for self-assembly (i.e., concentrations close the onset of aggregation) or the polydispersity in the lengths of the OEG chains. We have shown that the amount of unimer present could be modulated by either the content of common solvent or the selective solvent mixture. This alteration of the solvent system had a significant effect on the morphology of the supramolecular polymers.

We also observed that the amount of **PDI-1** material in the aggregated state increased after sonication. This increase was attributed to the sonication causing fragmentation of the long fibres, increasing the number of nuclei to which free unimer in the seed solution was able to add. This process had a significant impact on the kinetic stability of seeds and the length of fibres formed by seeded growth.

Finally, we reported the formation of more complex segmented supramolecular block copolymers by the addition of **PDI-1** monomers to chemically distinct seeds formed from **PDI-2**. Characterisation to distinguish the segments of the supramolecular block copolymers has not been possible to date. However, further work is in progress to expand and exploit this approach to produce chemically distinct functional block-like supramolecular structures for applications in optoelectronics, heterojunctions and to form hierarchically ordered supramolecular materials.

Experimental Section

Formation of PDI-1 fibres

PDI-1 was dissolved in $CHCl_3$ at 4.7×10^{-5} M to give a bright orange solution. To a 100 µL aliquot was added 900 µL of *i*PrOH. The solution was aged for several days at room temperature. A 10 µL aliquot was drop cast on a carbon-coated copper grid.

PDI-1 Seed formation

A 7 mL vial containing 1 mL of fibres in 9:1 *i*PrOH:$CHCl_3$ at 4.7×10^{-6} M was capped with a septum and sonicated for 10 minutes at 0 °C using a sonotrode.

Seeded growth of PDI-1 fibres

1 µg of seed solution (L_n = 61 nm, L_w/L_n = 1.24) in 100 µL 9:1 *i*PrOH:$CHCl_3$ was diluted in *i*PrOH and then (a) 2 µg, (b) 3 µg, (c) 4 µg, (d) 5 µg, (e) 6 µg, (f) 7 µg, (g) 8 µg, (h) 9 µg and (i) 10 µg of **PDI-1** in $CHCl_3$ at 4.7×10^{-5} M was added. The solutions were shaken and left to age for 24 h at room temperature. Multiple TEM images were obtained and the lengths of the fibres were measured for 200-220 fibres. Sample (i) was carried out in a cuvette and UV-vis absorption spectra were collected every 5 minutes for 60 minutes and then every 20 minutes for 1380 minutes.

Full experimental procedures, characterisation for all new compounds and copies of ^1H, ^{13}C NMR and MALDI ToF spectra are provided in the Supporting Information.

Acknowledgements

C. J-W thanks the Bristol Chemical Synthesis Centre for Doctoral Training, funded by the Engineering and Physical Sciences Research Council (EPSRC) for a Ph.D (EP/G036764/1). X.H. thanks the National Natural Science Foundation of China (No. 51703166) and National 1000-Plan Program for support**.** H. E. S. thanks the EPSRC for a Ph.D (EP/N509619/1). Mass spectrometric analysis was performed on instrumentation bought through the Core Capability for Chemistry Research - Strategic Investment in Mass Spectrometry EPSRC grant (EP/K03927X/1). PeakForce atomic force microscopy was carried out in the Chemical Imaging Facility, University of Bristol with equipment funded by EPSRC under "Atoms to Applications" Grant EP/K035746/1.

Keywords: Supramolecular polymer • Seeded growth • Perylene Diimide

[1] a) T. F. A. De Greef, M. M. J. Smulders, M. Wolffs, A. P. H. J. Schenning, R. P. Sijbesma, E. W. Meijer, *Chemical Reviews* **2009**, *109*, 5687-5754; b) R. P. Sijbesma, F. H. Beijer, L. Brunsveld, B. J. B. Folmer, J. H. K. K. Hirschberg, R. F. M. Lange, J. K. L. Lowe, E. W. Meijer, *Science* **1997**, *278*, 1601; c) T. Aida, E. W. Meijer, S. I. Stupp, *Science* **2012**, *335*, 813-817; d) C. Rest, R. Kandanelli, G. Fernandez, *Chemical Society Reviews* **2015**, *44*, 2543-2572; e) L. Yang, X. Tan, Z. Wang, X. Zhang, *Chemical Reviews* **2015**, *115*, 7196-7239; f) S. S. Babu, V. K. Praveen, A. Ajayaghosh, *Chemical Reviews* **2014**, *114*, 1973-2129; g) E. Busseron, Y. Ruff, E. Moulin, N. Giuseppone, *Nanoscale* **2013**, *5*, 7098-7140; h) J. Kang, D. Miyajima, T. Mori, Y. Inoue, Y. Itoh, T. Aida, *Science* **2015**, *347*, 646-651.

[2] J. Boekhoven, W. E. Hendriksen, G. J. M. Koper, R. Eelkema, J. H. van Esch, *Science* **2015**, *349*, 1075-1079.

[3] J. W. Sadownik, E. Mattia, P. Nowak, S. Otto, *Nat Chem* **2016**, *8*, 264-269.

[4] C. Frieden, *Protein Science* **2007**, *16*, 2334-2344.

[5] a) F. Würthner, C. R. Saha-Möller, B. Fimmel, S. Ogi, P. Leowanawat, D. Schmidt, *Chemical Reviews* **2016**, *116*, 962-1052; b) C. Huang, S. Barlow, S. R. Marder, *The Journal of Organic Chemistry* **2011**, *76*, 2386-2407; c) G. Echue, I. Hamley, G. C. Lloyd Jones, C. F. J. Faul, *Langmuir* **2016**, *32*, 9023-9032; d) C. F. J. Faul, *Accounts of Chemical Research* **2014**, *47*, 3428-3438; e) Y. Huang, Y. Yan, B. M. Smarsly, Z. Wei, C. F. J. Faul, *Journal of Materials Chemistry* **2009**, *19*, 2356-2362; f) Y. Huang, J. Hu, W. Kuang, Z. Wei, C. F. J. Faul, *Chemical Communications* **2011**, *47*, 5554-5556; g) C. Kulkarni, K. K. Bejagam, S. P. Senanayak, K. S. Narayan, S. Balasubramanian, S. J. George, *Journal of the American Chemical Society* **2015**, *137*, 3924-3932; h) E. Krieg, S. Albeck, H. Weissman, E. Shimoni, B. Rybtchinski, *PLOS ONE* **2013**, *8*, e63188; i) X. Feng, Y. An, Z. Yao, C. Li, G. Shi, *ACS Applied Materials & Interfaces* **2012**, *4*, 614-618.

[6] X. Zhang, Z. Chen, F. Würthner, *Journal of the American Chemical Society* **2007**, *129*, 4886-4887.

[7] X. Zhang, S. Rehm, M. M. Safont-Sempere, F. Würthner, *Nat Chem* **2009**, *1*, 623-629.

[8] Y. Zhang, C. Peng, Z. Zhou, R. Duan, H. Ji, Y. Che, J. Zhao, *Advanced Materials* **2015**, *27*, 320-325.

[9] S. Ghosh, X.-Q. Li, V. Stepanenko, F. Würthner, *Chemistry – A European Journal* **2008**, *14*, 11343-11357.

[10] X. Ma, Y. Zhang, Y. Zheng, Y. Zhang, X. Tao, Y. Che, J. Zhao, *Chemical Communications* **2015**, *51*, 4231-4233.

[11] Y. Liu, C. Peng, W. Xiong, Y. Zhang, Y. Gong, Y. Che, J. Zhao, *Angewandte Chemie International Edition* **2017**, *56*, 11380-11384.

[12] a) X. Zhan, A. Facchetti, S. Barlow, T. J. Marks, M. A. Ratner, M. R. Wasielewski, S. R. Marder, *Advanced Materials* **2011**, *23*, 268-284; b) J. E. Anthony, *Chemistry of Materials* **2011**, *23*, 583-590.

[13] a) F. Würthner, Z. Chen, F. J. M. Hoeben, P. Osswald, C.-C. You, P. Jonkheijm, J. v. Herrikhuyzen, A. P. H. J. Schenning, P. P. A. M. van der Schoot, E. W. Meijer, E. H. A. Beckers, S. C. J. Meskers, R. A. J. Janssen, *Journal of the American Chemical Society* **2004**, *126*, 10611-10618; b) L. Bu, E. Pentzer, F. A. Bokel, T. Emrick, R. C. Hayward, *ACS Nano* **2012**, *6*, 10924-10929; c) L. Bu, T. J. Dawson, R. C. Hayward, *ACS Nano* **2015**, *9*, 1878-1885.

[14] X. Li, P. J. Wolanin, L. R. MacFarlane, R. L. Harniman, J. Qian, O. E. C. Gould, T. G. Dane, J. Rudin, M. J. Cryan, T. Schmaltz, H. Frauenrath, M. A. Winnik, C. F. J. Faul, I. Manners, *Nature Communications* **2017**, *8*, 15909.

[15] a) R. D. Mukhopadhyay, A. Ajayaghosh, *Science* **2015**, *349*, 241-242; b) D. van der Zwaag, T. F. A. de Greef, E.

W. Meijer, *Angewandte Chemie International Edition* **2015**, *54*, 8334-8336; c) D. J. Lunn, J. R. Finnegan, I. Manners, *Chemical Science* **2015**, *6*, 3663-3673; d) J. Kumar, H. Tsumatori, J. Yuasa, T. Kawai, T. Nakashima, *Angewandte Chemie International Edition* **2015**, *54*, 5943-5947; e) B. Kemper, L. Zengerling, D. Spitzer, R. Otter, T. Bauer, P. Besenius, *Journal of the American Chemical Society* **2018**, *140*, 534-537; f) F. Tantakitti, J. Boekhoven, X. Wang, R. V. Kazantsev, T. Yu, J. Li, E. Zhuang, R. Zandi, J. H. Ortony, C. J. Newcomb, L. C. Palmer, G. S. Shekhawat, M. O. de la Cruz, G. C. Schatz, S. I. Stupp, *Nature Materials* **2016**, *15*, 469-476; g) J. Baram, H. Weissman, B. Rybtchinski, *The Journal of Physical Chemistry B* **2014**, *118*, 12068-12073; h) B. Li, S. Li, Y. Zhou, H. A. Ardona, L. R. Valverde, W. L. Wilson, J. D. Tovar, C. M. Schroeder, *ACS Applied Materials & Interfaces* **2017**, *9*, 3977-3984; i) H. A. M. Ardona, E. R. Draper, F. Citossi, M. Wallace, L. C. Serpell, D. J. Adams, J. D. Tovar, *Journal of the American Chemical Society* **2017**, *139*, 8685-8692.

[16] a) X. Wang, G. Guerin, H. Wang, Y. Wang, I. Manners, M. A. Winnik, *Science* **2007**, *317*, 644-647; b) J. Qian, X. Li, D. J. Lunn, J. Gwyther, Z. M. Hudson, E. Kynaston, P. A. Rupar, M. A. Winnik, I. Manners, *Journal of the American Chemical Society* **2014**, *136*, 4121-4124; c) R. L. N. Hailes, A. M. Oliver, J. Gwyther, G. R. Whittell, I. Manners, *Chemical Society Reviews* **2016**, *45*, 5358-5407; d) J. B. Gilroy, T. Gadt, G. R. Whittell, L. Chabanne, J. M. Mitchels, R. M. Richardson, M. A. Winnik, I. Manners, *Nature Chemistry* **2010**, *2*, 566-570; e) N. Petzetakis, A. P. Dove, R. K. O'Reilly, *Chemical Science* **2011**, *2*, 955-960; f) J. Schmelz, A. E. Schedl, C. Steinlein, I. Manners, H. Schmalz, *Journal of the American Chemical Society* **2012**, *134*, 14217-14225; g) M. C. Arno, M. Inam, Z. Coe, G. Cambridge, L. J. Macdougall, R. Keogh, A. P. Dove, R. K. O'Reilly, *Journal of the American Chemical Society* **2017**, *139*, 16980-16985; h) H. Qiu, Y. Gao, C. E. Boott, O. E. C. Gould, R. L. Harniman, M. J. Miles, S. E. D. Webb, M. A. Winnik, I. Manners, *Science* **2016**, *352*, 697-701; i) X. He, M.-S. Hsiao, C. E. Boott, R. L. Harniman, A. Nazemi, X. Li, M. A. Winnik, I. Manners, *Nat Mater* **2017**, *16*, 481-488.

[17] G. Guérin, H. Wang, I. Manners, M. A. Winnik, *Journal of the American Chemical Society* **2008**, *130*, 14763-14771.

[18] a) W. Zhang, W. Jin, T. Fukushima, A. Saeki, S. Seki, T. Aida, *Science* **2011**, *334*, 340-343; b) W. Zhang, W. Jin, T. Fukushima, T. Mori, T. Aida, *Journal of the American Chemical Society* **2015**, *137*, 13792-13795.

[19] a) S. Ogi, K. Sugiyasu, S. Manna, S. Samitsu, M. Takeuchi, *Nat Chem* **2014**, *6*, 188-195; b) S. Ogi, T. Fukui, M. L. Jue, M. Takeuchi, K. Sugiyasu, *Angewandte Chemie International Edition* **2014**, *53*, 14363-14367; c) T. Fukui, S. Kawai, S. Fujinuma, Y. Matsushita, T. Yasuda, T. Sakurai, S. Seki, M. Takeuchi, K. Sugiyasu, *Nat Chem* **2017**, *9*, 493-499.

[20] a) M. E. Robinson, D. J. Lunn, A. Nazemi, G. R. Whittell, L. De Cola, I. Manners, *Chemical Communications* **2015**, *51*, 15921-15924; b) M. E. Robinson, A. Nazemi, D. J. Lunn, D. W. Hayward, C. E. Boott, M.-S. Hsiao, R. L. Harniman, S. A. Davis, G. R. Whittell, R. M. Richardson, L. De Cola, I. Manners, *ACS Nano* **2017**, *11*, 9162-9175; c) A. Aliprandi, M. Mauro, L. De Cola, *Nature Chemistry* **2016**, *8*, 10-15.

[21] E. E. Greciano, L. Sánchez, *Chemistry – A European Journal* **2016**, *22*, 13724-13730.

[22] M. Endo, T. Fukui, S. H. Jung, S. Yagai, M. Takeuchi, K. Sugiyasu, *Journal of the American Chemical Society* **2016**, *138*, 14347-14353.

[23] L. H. Beun, L. Albertazzi, D. van der Zwaag, R. de Vries, M. A. Cohen Stuart, *ACS Nano* **2016**, *10*, 4973-4980.

[24] A. Pal, M. Malakoutikhah, G. Leonetti, M. Tezcan, M. Colomb-Delsuc, V. D. Nguyen, J. van der Gucht, S. Otto, *Angewandte Chemie International Edition* **2015**, *54*, 7852-7856.

[25] D. S. Pal, H. Kar, S. Ghosh, *Chemical Communications* **2018**, *54*, 928-931.

[26] J. S. Valera, R. Gómez, L. Sánchez, *Small* **2018**, *14*, 1702437-n/a.

[27] a) S. Ogi, V. Stepanenko, K. Sugiyasu, M. Takeuchi, F. Würthner, *Journal of the American Chemical Society* **2015**, *137*, 3300-3307; b) S. Ogi, V. Stepanenko, J. Thein, F. Würthner, *Journal of the American Chemical Society* **2016**, *138*, 670-678; c) W. Wagner, M. Wehner, V. Stepanenko, S. Ogi, F. Würthner, *Angewandte Chemie International Edition* **2017**, *56*, 16008-16012.

[28] X. Ma, Y. Zhang, Y. Zhang, Y. Liu, Y. Che, J. Zhao, *Angewandte Chemie International Edition* **2016**, *55*, 9539-9543.

[29] a) H. Frisch, E. C. Fritz, F. Stricker, L. Schmuser, D. Spitzer, T. Weidner, B. J. Ravoo, P. Besenius, *Angewandte Chemie International Edition* **2016**, *55*, 7242-7246; b) B. Adelizzi, A. Aloi, A. J. Markvoort, H. M. M. Ten Eikelder, I. K. Voets, A. R. A. Palmans, E. W. Meijer, *Journal of the American Chemical Society* **2018**, *140*, 7168-7175.

[30] X. Zhang, D. Görl, V. Stepanenko, F. Würthner, *Angewandte Chemie International Edition* **2014**, *53*, 1270-1274.

[31] M. M. J. Smulders, M. M. L. Nieuwenhuizen, T. F. A. de Greef, P. van der Schoot, A. P. H. J. Schenning, E. W. Meijer, *Chemistry – A European Journal* **2010**, *16*, 362-367.

[32] a) F. Würthner, C. Thalacker, S. Diele, C. Tschierske, *Chemistry – A European Journal* **2001**, *7*, 2245-2253; b) O. A. Bell, G. Wu, J. S. Haataja, F. Brömmel, N. Fey, A. M. Seddon, R. L. Harniman, R. M. Richardson, O. Ikkala, X. Zhang, C. F. J. Faul, *Journal of the American Chemical Society* **2015**, *137*, 14288-14294; c) G. Echue, G. C. Lloyd-Jones, C. F. J. Faul, *Chemistry – A European Journal* **2015**, *21*, 5118-5128.

[33] M. M. J. Smulders, A. P. H. J. Schenning, E. W. Meijer, *Journal of the American Chemical Society* **2008**, *130*, 606-611.

[34] G. Rizis, T. G. M. van de Ven, A. Eisenberg, *Angewandte Chemie International Edition* **2014**, *53*, 9000-9003.

10.1002/chem.201801424

WILEY-VCH

FULL PAPER

We demonstrate the controlled solution self-assembly of an amphiphilic perylene diimide, with a hydrophobic perylene core and hydrophilic imide substituents with polydisperse oligo(ethyleneglycol) tethers. It was possible, by a seeded-growth mechanism, to form colloidally stable, one-dimensional fibres with controllable lengths and low dispersities.

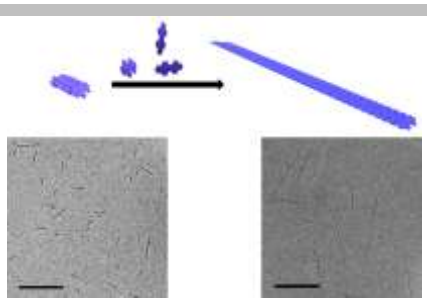

*Charles Jarrett-Wilkins, Xiaoming He, Henry E. Symons, Robert L. Harniman, Charl F. J. Faul, * Ian Manners**

Page No. – Page No.

Living Supramolecular Polymerisation of Perylene Diimide Amphiphiles by Seeded Growth under Kinetic Control

[a] Title(s), Initial(s), Surname(s) of Author(s) including Correspon
Author(s)
Department
Institution
Address 1
E-mail:
[b] Title(s), Initial(s), Surname(s) of Author(s)
Department
Institution
Address 2

Supporting information for this article is given via a link at the the document.((Please delete this text if not appropriate))